On the Suicidal Pedestrian Differential Game

Ioannis Exarchos, Panagiotis Tsiotras & Meir Pachter

Dynamic Games and Applications

ISSN 2153-0785
Volume 5
Number 3

Dyn Games Appl (2015) 5:297-317
DOI 10.1007/s13235-014-0130-2

Springer

Dyn Games Appl (2015) 5:297–317
DOI 10.1007/s13235-014-0130-2

On the Suicidal Pedestrian Differential Game

Ioannis Exarchos · Panagiotis Tsiotras · Meir Pachter

Published online: 2 December 2014

Abstract We consider the following differential game of pursuit and evasion involving two participating players: an evader, which has limited maneuverability, and an agile pursuer. The agents move on the Euclidean plane with different but constant speeds. Whereas the pursuer can change the orientation of its velocity vector arbitrarily fast, that is, he is a "pedestrian" á la Isaacs, the evader cannot make turns having a radius smaller than a specified minimum turning radius. This problem can be seen as a reversed Homicidal Chauffeur game, hence the name "Suicidal Pedestrian Differential Game." The aim of this paper is to derive the optimal strategies of the two players and characterize the initial conditions that lead to capture if the pursuer acts optimally, and areas that guarantee evasion regardless of the pursuer's strategy. Both proximity-capture and point-capture are considered. After applying the optimal strategy for the evader, it is shown that the case of point-capture reduces to a special version of Zermelo's Navigation Problem (ZNP) for the pursuer. Therefore, the well-known ZNP solution can be used to validate the results obtained through the differential game framework, as well as to characterize the time-optimal trajectories. The results are directly applicable to collision avoidance in maritime and Air Traffic Control applications.

Keywords Pursuit–evasion · Game of two cars · Zermelo's navigation problem

I. Exarchos · P. Tsiotras (✉)
Department of Aerospace Engineering, Georgia Institute of Technology, Atlanta, GA 30332-0150, USA
e-mail: tsiotras@gatech.edu

I. Exarchos
e-mail: exarchos@gatech.edu

M. Pachter
Department of Electrical and Computer Engineering, Air Force Institute of Technology, Wright-Patterson A.F.B., OH 45433, USA
e-mail: Meir.Pachter@afit.edu

1 Introduction

The literature on differential/dynamic games of pursuit and evasion is extensive. An interesting discussion on the historical background of problems of pursuit and evasion can be found in [20]. Isaacs [9], in his seminal work on the extension of game theory to the framework of differential games, studied several examples of pursuit and evasion. In the classical paper [8], the authors examined conditions under which capture is possible in a two-player linear-quadratic pursuit–evasion game: if both players are subject to single integrator dynamics and have no control constraints, then the necessary and sufficient condition for interception is that the speed of the pursuer is higher than that of the evader.

There are several special cases of two-player pursuit–evasion scenarios, including restrictions on the space where the agents can move (e.g., [23], and the Lion and Man problem [30]), or problems with stochastic dynamics (see, for example, [32]). Two-player pursuit–evasion with curvature constraints were addressed in Isaacs' Homicidal Chauffeur problem [9,13] and the Game of Two Cars [14]. For the stochastic versions of these games see [25] and [33], respectively. A general solution for problems of restricted player maneuverability was presented in [6], wherein necessary and sufficient conditions for capture, regardless of the initial conditions of the players, were derived. Reference [6] states that a pursuer is guaranteed to capture the evader regardless of initial conditions only if she is faster than the evader, and does not have a major maneuverability disadvantage against the evader. These results were extended for motion in the three-dimensional space in [28]. Regardless of whether maneuverability restrictions are considered or not, the conditions leading to capture may be relaxed at the expense of including more pursuers in the game (see for example [4,27]).

In this paper, we consider an asymmetric version of the Game of Two Cars [14]. In the original formulation of the problem, both players have the same speed and the same maneuverability restrictions, i.e., they are identical, and capture occurs when the distance between the players becomes less than a constant, which is known as the "kill zone." The Game of Two Cars has been extensively studied in the literature. As with any pursuit–evasion game in which different initial conditions lead to different game outcomes, an essential part of the solution of the game is the determination of the *barrier* [9]. Simply put, the barrier is the surface that separates initial states of the game that lead to capture under optimal play, from states in which capture is impossible, as long as the evader plays optimally, and evasion is guaranteed. Further details on the concept of the barrier can be found in [24]. The barrier surface is in fact a *semipermeable surface*, that is, a surface whose crossing can be instigated only by suboptimal player action. An interesting fact concerning families of semipermeable surfaces is that they are determined solely by the motion dynamics and the imposed control constraints [10]. Thus, differential games sharing the same dynamics exhibit common families of semipermeable surfaces, regardless of their target set and outcome functional. In the case of Homicidal Chauffeur dynamics, such as in the present paper, those families have been identified in [26], where a numerical algorithm for the calculation of the Value function level sets is proposed. The approach in [26] is quite general and captures several variations of the problem. However, as shown in this paper, such a numerical approach is not necessary for our problem since the barrier surface can be computed in closed form.

The ramifications of the results that emerged from the analysis of the Game of Two Cars in applications of collision avoidance have been recognized in [18]. Their usefulness as analytic solutions to validate numerical algorithms was also highlighted in [19]. Several extensions and generalizations of this game appear in the literature under the name *maritime collision avoidance* [3,15–17,21,22,31]. In this game setting, the two agents have different constant speeds and different minimum turning radii. Analytic expressions for the barriers do exist

[17], but practical implementation is problematic because of the underlying assumptions: the exact maneuvering capability of the opponent is assumed to be known a priori, and a continuous measurement of her instantaneous orientation is also necessary.

Motivated by these technical difficulties, in this paper, we propose the investigation of the following variation of the Game of Two Cars, termed herein as the Suicidal Pedestrian Game: the two agents move with different constant speeds, and the evader is subject to maneuverability restrictions, while the pursuer is assumed to be completely agile. This leads to a game state of reduced dimensionality that utilizes the least amount of information on the characteristics of the pursuing agent. In this setting, the case in which the pursuer is not just more agile, but also faster than the evader, results in global capturability, i.e., the pursuer is always able to capture the evader regardless of the initial relative positioning of the agents [6]. We will therefore focus our analysis mainly on the more interesting case in which the evader is at least as fast as the pursuer. Furthermore, since the pursuer can change her orientation arbitrarily fast, the only target set that makes sense in this case is a circular target set, i.e., a circular "kill zone." This target set is collocated with the evader's instantaneous position. One can view this problem also as an inverse to the classical Homicidal Chauffeur problem, wherein the pursuer is faster but has maneuverability restrictions, and attempts to intercept a completely agile but slower evader by bringing her into her "kill zone." The title of the paper is inspired by this "role reversal" in the Homicidal Chauffeur game. The results of this paper are directly applicable to maritime collision avoidance and to Air Traffic Control, in the sense that a safe region around ownship is delineated such that it is guaranteed that, even in the worst case scenario of malicious behavior, a collision is avoidable.

During the review process, two little-known, scarcely cited papers [12,29] were brought to our attention. The first one treats the same problem as the one in this paper as a special case of the Game of Two Cars and presents a purely geometric procedure to obtain a solution. It thus avoids use of Isaacs' method and does not offer an analytic expression for the barrier. The same game is also briefly discussed in Appendix I of [29], which focuses on the investigation of feedback control laws for the pursuer. No detailed analysis of the game is offered however. Our paper, on the other hand, provides a complete analysis of the game, including the case of point-capture. Furthermore, an interesting connection with the classical Zermelo navigation problem from optimal control theory is given. This problem thus offers a rare instance where a complete, closed form, solution of a differential game can be provided.

The rest of the paper is organized as follows: In Sect. 2 we formally define the problem to be investigated. Next, in Sect. 3 we cast the problem within a differential game framework. The solution of the game provides us with an analytic expression for the barrier. In the same section, we also derive the optimal strategy of the evader, a policy which, unlike in the case of the Homicidal Chauffeur game, will turn out to be independent of the problem parameters. The special case of equal speeds for the two agents, as well as the special case in which the pursuer's capture radius is zero, i.e., *point-capture* is also considered. In Sect. 4, we turn our attention to the investigation of the characteristics of the *time-optimal* trajectories along with the corresponding agent strategies, that lead to point-capture. Sect. 4 also highlights the connection of the Suicidal Pedestrian Differential Game to the well-known *Zermelo Navigation Problem* from optimal control theory [5,34]. By applying Zermelo's navigation law, the analytic expression of the barrier in Sect. 3 is validated and, in addition, the complete family of time-optimal trajectories that lead to point-capture is obtained. Section 5 offers some insight on the characteristics of time-optimal trajectories when viewed from the inertial reference and Sect. 6 delineates the characteristics of trajectories in the case of pursuer superiority in both speed and maneuverability. Finally, Sect. 7 summarizes the results of the paper.

2 Problem Statement

Consider two players, a pursuer and an evader, moving on the Euclidean plane. The subscripts p and e will be reserved for the "Pursuer" (P) and the "Evader" (E), respectively. The pursuer's objective is *capture*, that is, interception of the evader in finite time, whereas the evader's objective is *evasion*, a state in which she avoids interception indefinitely. Interception occurs when the separation of the agents becomes smaller than a constant, ℓ, known as the radius of the pursuer's kill zone. The special case $\ell = 0$ corresponds to *point-capture*. The agents have different constant speeds, namely v_e, v_p, for the evader and the pursuer, respectively. We define $\alpha = v_p/v_e$ to be the *speed ratio*. The pursuer is assumed to be agile, in the sense that she can change the orientation of her velocity vector instantaneously. On the other hand, the evader is less agile and cannot make turns that have a radius smaller than his minimum turning radius R. In this setup, it is a well-known fact that if the pursuer moves with greater speed than the evader, then she will always be able to capture her opponent regardless of the initial relative positioning of the agents [6]. We will therefore restrict our analysis to the interesting case in which $\alpha \leq 1$, that is, $v_p \leq v_e$. The case $\alpha > 1$, in which global capturability of the evader is ensured, is discussed in Sect. 6.

The equations of motion for the pursuer and the evader, written in an inertial frame of reference with coordinates x and y, are given by

$$\dot{x}_p = v_p \cos\phi_p, \tag{1}$$

$$\dot{y}_p = v_p \sin\phi_p, \tag{2}$$

$$\dot{x}_e = v_e \cos\phi_e, \tag{3}$$

$$\dot{y}_e = v_e \sin\phi_e, \tag{4}$$

$$\dot{\phi}_e = -\frac{v_e}{R}u, \qquad u \in [-1, 1], \tag{5}$$

where the control u determines the evader's turn direction (left/negative or right/positive) and turn rate magnitude. The *Line of Sight* (LOS) is defined as the line connecting the pursuer and evader instantaneous positions. We wish to investigate the conditions under which capture is possible by obtaining a characterization of initial conditions that lead to capture, as opposed to initial conditions that lead to evasion under optimal play of both agents, and derive the corresponding optimal state feedback strategies for both P and E.

3 Differential Game Formulation and Solution

In order to determine which initial states lead to capture and which initial states lead to evasion under optimal play by both agents, we turn to the theory of differential games [9]. The answer to this question is obtained through the solution of a *game of kind*. Whenever the state space of a game is comprised of both types of initial conditions, that is, starting points that lead to evasion and starting points that lead to capture, under optimal play of both agents, there exists a surface which separates these two regions, called the barrier. This barrier is obtained by solving a game of kind. In a game of kind, the game outcome is essentially an event (in our case, capture or evasion), and, corresponding to whether or not this event occurs, the game payoff assumes discrete values. In contrast, in a *game of degree*, the payoff assumes a continuum of numerical values (e.g., how much time P needs in order to intercept E). For a more detailed presentation, as well as several examples for both types of games, the reader is referred to [9]. In this paper, we propose to cast the problem as a differential game of kind. For an alternative characterization of the problem as one of degree, see [7].

3.1 Differential Game

Recall that the equations of motion for the pursuer and the evader, written in an inertial frame of reference are given by Eqs. (1) through (5). It is easy to show [9] that one can transform the problem from the previous fifth-dimensional *realistic game space* to a two-dimensional *reduced game space*, by fixing the origin of a rotating coordinate frame at E's current position and by aligning the y-axis with E's velocity vector; see Fig. 1. The evader action then consists of choosing her center of curvature at a point $C = (R/u, 0)$ on the x-axis as shown in Fig. 1. Consequently, the reduced game space has only two states, namely the (x, y) position of P relative to E in the evader's fixed, velocity-aligned rotating frame. The equations of motion of P in this rotating frame are given by

$$\dot{x} = -\frac{v_e}{R} yu - v_p \sin\phi, \tag{6}$$

$$\dot{y} = \frac{v_e}{R} xu - v_e - v_p \cos\phi, \qquad u \in [-1, 1], \tag{7}$$

where ϕ is the pursuer's relative heading in this new reference frame, given by $\phi \triangleq \pi - \phi_p + \phi_e$.

We thus formally define the state vector of the game to be $\mathbf{x} = (x, y)^\mathsf{T}$. The game terminates when capture occurs, that is, when the relative distance between the evader and the pursuer becomes less than ℓ. The manifold contained within the game space which, once penetrated, signals the game termination is called the *terminal surface*. The terminal surface for our game is a circle with radius ℓ centered at the origin, i.e., the evader's position. We may thus formally define the terminal surface by $\mathcal{C} \triangleq \left\{\mathbf{x} \in \mathbb{R}^2 : |\mathbf{x}| = \ell\right\}$. Initializing the game within this circle leads to the trivial case when capture has already been accomplished. Hence, we focus our investigation on initial conditions that lie outside the circle, defining the game space as $\mathcal{E} \triangleq \left\{\mathbf{x} \in \mathbb{R}^2 : |\mathbf{x}| \geq \ell\right\}$. The terminal surface is then the boundary of the game space.

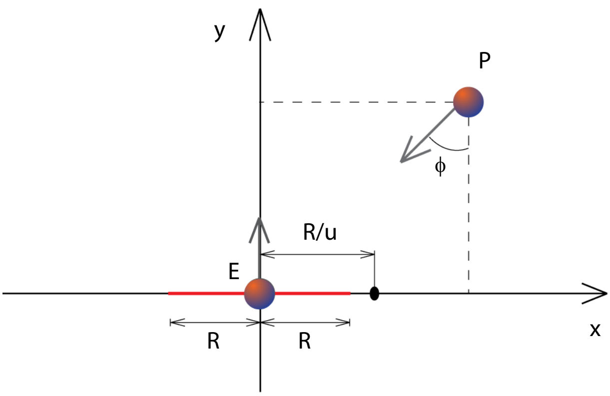

Fig. 1 The reduced state space. The reference frame is fixed on E's current position with the y-axis aligned along E's velocity vector. The evader's control action is equivalent to choosing her center of rotation $C = (R/u, 0)$ on the x-axis. A rotation of E around C has the same effect as a rotation of P around C with the same angular velocity, but in the opposite direction

Retaining the concept of the payoff as it appears in the theory of zero-sum games, we assign the values $+1$ for escape (termination does not occur) and -1 for capture (termination occurs, i.e., the circle is penetrated by the pursuer's trajectory). An additional step is necessary in the process of constructing the barrier of the game. Namely, we need to distinguish the critical case in which the state $\mathbf{x}$ reaches the terminal surface but does *not* cross it, ultimately returning back into the interior of $\mathcal{E}$. The case when the terminal surface is reached without penetration, is referred to as *neutral* outcome [9], and the corresponding payoff is assigned zero value. Thus, given an initial state $\mathbf{x}(t_0)$ at $t = t_0$ and the pursuer and evader control histories, $\phi(\cdot)$ and $u(\cdot)$ respectively, the payoff formally reads as

$$J(\mathbf{x}(t_0), \phi(\cdot), u(\cdot)) = \begin{cases} +1, & \text{for no termination (escape)}, \\ 0, & \text{neutral outcome}, \\ -1, & \text{for termination (capture)}. \end{cases} \tag{8}$$

We thus seek to solve the problem of conflicting actions represented by u (maximizing control) and ϕ (minimizing control) that maximize/minimize the payoff (8) under the dynamic equations (6) and (7). Our goal is to obtain an analytic expression for the barrier surface, which consists of all starting points that lead to the neutral outcome.

3.2 Solution of the Game

In order to solve the game defined above, we apply the framework developed in [9]. Since the game is clearly symmetric with respect to the y-axis, we will focus our analysis on the right-half plane $\{\mathbf{x} \in \mathcal{E} : x \geq 0\}$. The first step is to obtain the *usable part* of the terminal surface $\mathcal{C}$. It is not uncommon for a terminal surface of a game to be divided into two regions: the *Usable Part (UP)* and the *Nonusable Part*, which are separated by what is known in the literature as the *Boundary of the Usable Part (BUP)*. The usable part is the subset of the terminal surface on which the pursuer can enforce capture, namely, penetration of the terminal surface. The nonusable part is the remaining part of the terminal surface. On it, the game would end only if the evader does not play optimally. Essentially, no retrograde optimal paths exist emanating from the nonusable part (see [9] for an interesting discussion on these concepts, and [13,14] for further examples). The BUP separates the points on $\mathcal{C}$ (rather, infinitesimally close to $\mathcal{C}$) where immediate capture ensues, from those leading to immediate escape.

In order to identify the usable part of the terminal surface, let $\gamma \triangleq [\gamma_1\ \gamma_2]^\mathsf{T}$ be the unit vector normal to $\mathcal{C}$ from point $\mathbf{x}$ on $\mathcal{C}$, pointing into the interior of $\mathcal{E}$. Then, the usable part of $\mathcal{C}$ is the region in which the following (strict) inequality holds [9]:

$$\min_{\phi} \max_{u} \sum_{i=1}^{2} \gamma_i f_i(\mathbf{x}, u, \phi) < 0, \qquad \mathbf{x} \in \mathcal{C}, \tag{9}$$

where f_i $(i = 1, 2)$ denotes the right-hand-side of the differential equations (6) and (7), respectively (for our problem, $\mathbf{x}_1 = x$ and $\mathbf{x}_2 = y$). The nonusable part has the inequality sign reversed, and the BUP satisfies (9) as an equality. Parameterizing the terminal surface with the variable s as shown in Fig. 2, one readily obtains

$$(x, y) = (\ell \sin s, \ell \cos s), \qquad \mathbf{x} \in \mathcal{C}. \tag{10}$$

Since we restrict the analysis in the right-half plane, the angle s assumes values between zero and π. The expression for γ therefore becomes

$$\gamma = (\sin s, \cos s). \tag{11}$$

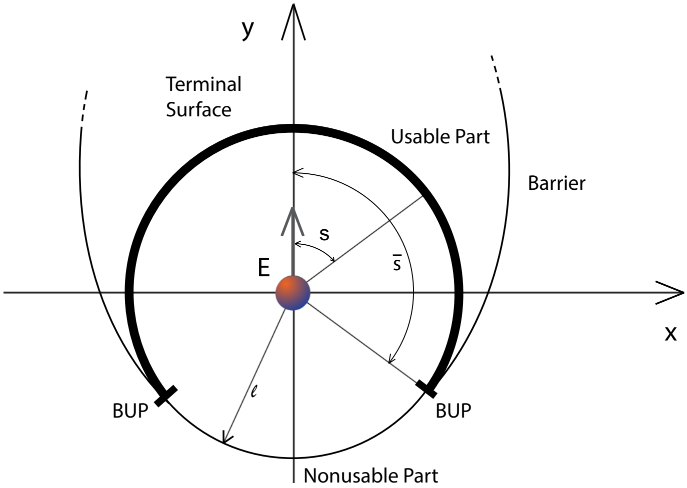

Fig. 2 The terminal surface $\mathcal{C}$ of the game, which is a *circle* of radius ℓ. It is divided into the usable part (the *dark line*) and the nonusable part, separated by the BUP. The BUP connects to the barrier, which meets the terminal surface at the BUP tangentially

In light of the above, and by virtue of the dynamics (6), (7), Eq. (9) yields

$$\min_{\phi}\max_{|u|\leq 1}\left\{\left(-\frac{v_e}{R}y\sin s+\frac{v_e}{R}x\cos s\right)u + (-v_p\sin\phi\sin s - v_e\cos s - v_p\cos\phi\cos s)\right\} < 0, \quad \mathbf{x}\in\mathcal{C}. \tag{12}$$

Substitution of the parameterization (10) in Eq. (12) causes the coefficient of u to vanish. It follows that the usable part of the terminal surface is the same, regardless of the evader's control strategy. This is merely a manifestation of the fact that the evader's dynamics are nonholonomic.

We are therefore left with the expression

$$\min_{\phi}\left\{-v_p\sin\phi\sin s - v_e\cos s - v_p\cos\phi\cos s\right\} < 0, \tag{13}$$

which may be rewritten as

$$\min_{\phi}\{-\cos(\phi - s)\} < \frac{v_e}{v_p}\cos s. \tag{14}$$

The left-hand-side of the above equation is minimized for $\phi^* = s$, having the value -1. The usable part of the terminal surface is therefore specified by

$$\cos s > -\frac{v_p}{v_e}, \qquad s\in\left(\frac{\pi}{2},\pi\right], \tag{15}$$

and the BUP is thus determined through

$$\bar{s} = \arccos(-\frac{v_p}{v_e}), \qquad \bar{s}\in\left(\frac{\pi}{2},\pi\right]. \tag{16}$$

An illustration of the usable part, the BUP and the nonusable part is given in Fig. 2.

Having identified the BUP, we turn our attention to the construction of the barrier. The barrier is a *semipermeable surface* [9], that is, optimal play by both agents starting from any point will generate a trajectory that does not penetrate this surface. Let $\mathcal{S}$ be such a surface in $\mathcal{E}$ and assume it is smooth, and at each of its points let $\nu \triangleq [\nu_1\ \nu_2]^\mathsf{T}$ be its normal vector of unit length, extending into the escape zone.

The *Isaacs equation* for games of kind then formally reads

$$\min_{\phi} \max_{u} \left[\sum_{i=1}^{2} \nu_i f_i(\mathbf{x}, u, \phi) \right] = 0, \qquad \mathbf{x} \in \mathcal{S}. \tag{17}$$

The Isaacs equation essentially states that on a semipermeable surface, such as the barrier, the vector field of the dynamics, after optimal controls have been applied, is tangent to that surface. Therefore, no penetration of that surface can occur under optimal play. Equation (17) can be rewritten, for the problem at hand, as follows:

$$\min_{\phi} \max_{|u|\leq 1} \left[-\frac{v_e}{R}(y\nu_1 - x\nu_2)u - v_p(\nu_1 \sin\phi + \nu_2 \cos\phi) - v_e \nu_2 \right] = 0, \quad \mathbf{x} \in \mathcal{S}. \tag{18}$$

Introducing the reverse time variable $\tau = t_f - t$, where t_f is the time of game termination, we define the following functions of the retrograde time:

$$A(\tau) \triangleq y\nu_1 - x\nu_2, \tag{19}$$

$$\sigma(\tau) \triangleq \operatorname{sign}(A(\tau)), \tag{20}$$

$$c(\tau) \triangleq \frac{v_e}{R}\sigma(\tau), \tag{21}$$

and proceed to the calculation of the optimal controls from (18). Since $u \in [-1, 1]$, it follows from (18) that

$$u^*(\tau) = -\operatorname{sign}(A(\tau)) = -\sigma(\tau), \tag{22}$$

which implies that E's optimal control is *bang-bang*. Furthermore, applying the Lemma on Circular Vectograms [9] in (18) for the minimization of the term $-(\nu_1 \sin\phi + \nu_2 \cos\phi)$ in terms of ϕ, yields the optimal action for the pursuer, as follows:

$$\cos\phi^*(\tau) = \nu_2, \qquad \sin\phi^*(\tau) = \nu_1. \tag{23}$$

Thus, Eq. (18) becomes

$$c(\tau)A(\tau) - v_p - v_e\nu_2(\tau) = 0, \qquad \mathbf{x} \in \mathcal{S}. \tag{24}$$

The next step is to derive the *Retrogressive Path Equations* [9]. These are the equations arising when one solves the game backwards in time, starting from the usable part of the terminal surface $\mathcal{C}$. Denoting with $(^\circ)$ the derivative with respect to τ, the retrograde evolution of the vector ν can be calculated as

$$\mathring{\nu}_j = \sum_{i=1}^{2} \nu_i \frac{\partial f_i(\mathbf{x}, \phi^*, u^*)}{\partial \mathbf{x}_j}, \qquad j = 1, 2. \tag{25}$$

One readily concludes from (25) and (6), (7) that

$$\mathring{\nu}_1 = -c\nu_2 \tag{26}$$

$$\mathring{\nu}_2 = c\nu_1. \tag{27}$$

The retrogressive path equations for the game states can be established if one applies the optimal controls u^* and ϕ^* in Eqs. (6) and (7) and switches the sign to reverse the time flow:

$$\overset{\circ}{x} = -cy + v_p \nu_1, \tag{28}$$

$$\overset{\circ}{y} = cx + v_e + v_p \nu_2. \tag{29}$$

A critical point now is to connect the barrier to the terminal surface. Recalling the definitions of the barrier and the BUP, it is evident that they are connected [9]; the barrier extends from the BUP of $\mathcal{C}$ into $\mathcal{E}$. Furthermore, since the vector field is tangential to the barrier, and no penetration of $\mathcal{C}$ occurs at the BUP, the two surfaces meet tangentially (see Fig. 2) . This last statement essentially translates into ν being parallel to γ, and thus we may take

$$\nu = \gamma, \qquad \mathbf{x} \in \mathcal{C} \cap \mathcal{S}. \tag{30}$$

Recall that the function $A(\tau)$ in (19) determines the sign of the optimal evader control. The inverse evolution of A is given by direct application of the ($\circ$) operator in the definition of A

$$\overset{\circ}{A} = y\overset{\circ}{\nu}_1 + \overset{\circ}{y}\nu_1 - x\overset{\circ}{\nu}_2 - \overset{\circ}{x}\nu_2,$$

which, after applying the expressions for $\overset{\circ}{\nu}_1$, $\overset{\circ}{\nu}_2$, $\overset{\circ}{x}$ and $\overset{\circ}{y}$, simplifies to

$$\overset{\circ}{A} = \nu_1 v_e. \tag{31}$$

Therefore, and since $A \equiv 0$ on $\mathcal{C}$, the sign of A sufficiently close to the terminal surface is determined by $\overset{\circ}{A}$, or

$$\sigma = \text{sign}(\nu_1 v_e) = \text{sign}(\gamma_1) = \text{sign}(\sin s) = \text{sign}(s) = 1, \tag{32}$$

where we have used the parameterization of γ_1 given by (11). This implies that

$$c = \frac{v_e}{R}, \tag{33}$$

and

$$u^* = -1. \tag{34}$$

The evader's optimal strategy when P is close to $\mathcal{C}$ is therefore established: E will try to steer away from P with his maximum turning capability $u^* = -1$, in an attempt to eliminate the velocity vector component pointing toward P as fast as possible. The evader's strategy is depicted in Fig. 3.

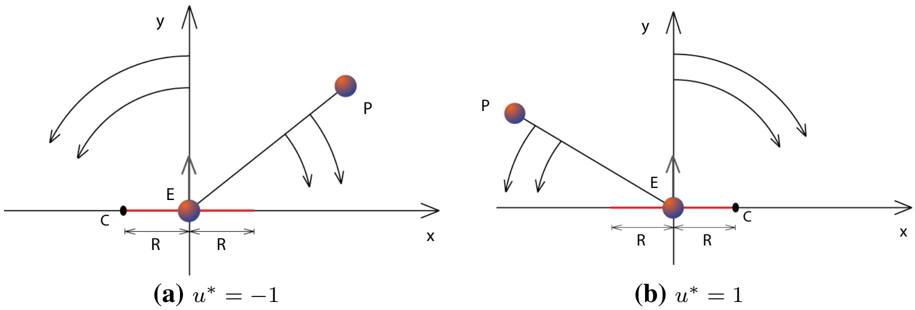

Fig. 3 Optimal evader strategies **a** for $x > 0$ and **b** for $x < 0$, by virtue of the symmetry of the problem. The *arrows* indicate the corresponding rotation of the LOS and the reference frame

To obtain the boundary conditions for the retrogressive equations for the barrier, we investigate their values on the BUP. Recalling the s-parameterization of $\mathcal{C}$ and the particular value $\bar{s}$ for the BUP given by (16), we obtain the boundary conditions

$$x(\tau = 0) = \ell \sin \bar{s}, \tag{35}$$
$$y(\tau = 0) = \ell \cos \bar{s}, \tag{36}$$
$$\nu_1(\tau = 0) = \sin \bar{s}, \tag{37}$$
$$\nu_2(\tau = 0) = \cos \bar{s}. \tag{38}$$

Thus, we are now able to integrate the system of Eqs. (26)–(29) subject to the above boundary conditions, and readily obtain

$$\nu_1(\tau) = \sin(\bar{s} - c\tau), \tag{39}$$
$$\nu_2(\tau) = \cos(\bar{s} - c\tau), \qquad \tau \in [0, \tau_{\max}]. \tag{40}$$

The above equations remain valid up until the time instant $\tau_{\max}$ is reached, defined in Eq. (43) below. The analytic expression of the barrier curve is

$$x(\tau) = -R + R\cos(c\tau) + (\ell + v_p\tau)\sin(\bar{s} - c\tau), \tag{41}$$
$$y(\tau) = R\sin(c\tau) + (\ell + v_p\tau)\cos(\bar{s} - c\tau), \qquad \tau \in [0, \tau_{\max}], \tag{42}$$

where $\bar{s}$ is given by (16). Equations (41) and (42) define the *barrier* of the game, that is, they separate the game space into two regions; a region in which optimal play of the pursuer leads to capture and a region in which optimal play of the evader leads to evasion. To obtain $\tau_{\max}$, it is important to note that the barrier expression is invalidated as soon as two barrier branches intersect – the part of the barrier arc beyond the point of intersection is then no longer valid and is therefore discarded. In our case, the two branches of the barrier intersect on the y-axis, because of the inherent symmetry of the problem at hand. Thus, we may obtain $\tau_{\max}$ as the root of $x(\tau) = 0$, i.e., $\tau_{\max}$ is the solution of the transcendental equation:

$$(\ell + v_p\tau_{\max})\sin(\bar{s} - c\tau_{\max}) = R - R\cos(c\tau_{\max}). \tag{43}$$

Figure 4 depicts the barrier for $v_e = 1$, $v_p = 0.6$, $R = 0.7$, $\ell = 0.5$. Notice that the barrier meets the terminal surface at the BUP tangentially.

Remark 1 It may happen that the game is initiated with a state that lies on the y-axis. In this case, the evader's control is not uniquely determined. In fact, the positive y-axis is a particular type of singular surface for this game, called the *dispersal* surface [9]. Around a dispersal surface, the state is driven away from it by the evader's control input. Starting from a state on a dispersal surface, there is ambiguity in E's optimal control; it is also the only locus on which E's optimal response is not independent of P's action. This is commonly known as *perpetuated dilemma*, a problem, which is usually eliminated by allowing agents to randomize their actions. On the dispersal surface, the pursuer will give the evader a small temporal advantage by slightly delaying his action, and thus, although lengthening a bit the time to capture, cause the state to move away from the dispersal surface. The evader, having chosen a direction, will be captured by the pursuer, albeit a bit later.

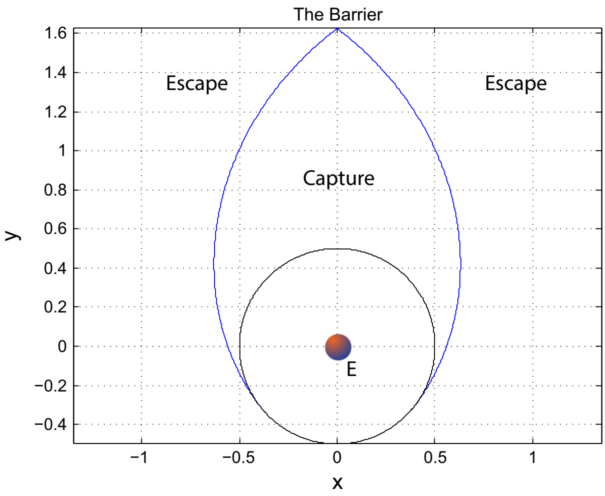

Fig. 4 The barrier, given by Eqs. (41) and (42), for $v_e = 1$, $v_p = 0.6$, $R = 0.7$, $\ell = 0.5$. Notice that the barrier meets the terminal surface tangentially at the BUP

3.3 The Case of Equal Speeds

The solution for the case in which both agents have the same speed may be obtained directly from the preceding analysis by applying $v_e = v_p = v$. The BUP in this case is

$$\bar{s} = \arccos\left(-\frac{v_p}{v_e}\right) = \pi, \tag{44}$$

which means that the entire terminal surface is usable, except for the lowest point of the capture circle. The barrier is obtained by direct substitution of $\bar{s} = \pi$ in Eqs. (41), (42):

$$x(\tau) = -R + R\cos(c\tau) + (\ell + v\tau)\sin(c\tau), \tag{45}$$

$$y(\tau) = R\sin(c\tau) - (\ell + v\tau)\cos(c\tau), \qquad \tau \in [0, \tau_{\max}], \tag{46}$$

where $\tau_{\max}$ is now the solution to the transcendental equation:

$$(\ell + v\tau_{\max})\sin(c\tau_{\max}) = R - R\cos(c\tau_{\max}). \tag{47}$$

The barrier is tangent to the bottom of the capture circle, as shown in Fig. 5. Recall that when the pursuer is faster than the evader, capturability is global and a barrier does not exist. The case when the speed ratio is equal to one is in fact the first instance where a barrier appears, and the pursuer's bounded capture zone is then maximal; as the speed ratio v_p/v_e becomes less than one, the bounded capture zone shrinks.

3.4 The Case of Point-Capture

The solution of the case of point-capture can be obtained by direct substitution of $\ell = 0$ in the barrier expressions (41) and (42), which leads to

$$x(\tau) = -R + R\cos(c\tau) + v_p\tau\sin(\bar{s} - c\tau), \tag{48}$$

$$y(\tau) = R\sin(c\tau) + v_p\tau\cos(\bar{s} - c\tau), \qquad \tau \in [0, \tau_{\max}], \tag{49}$$

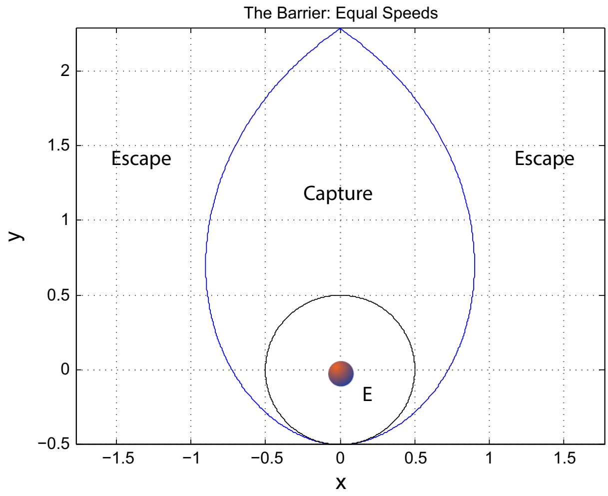

Fig. 5 The barrier, given by Eqs. (45) and (46) for the case of equal speeds $v_e = v_p = 1$, $R = 0.7$, $\ell = 0.5$. The barrier meets the terminal surface at the BUP tangentially at the bottom of the capture *circle*

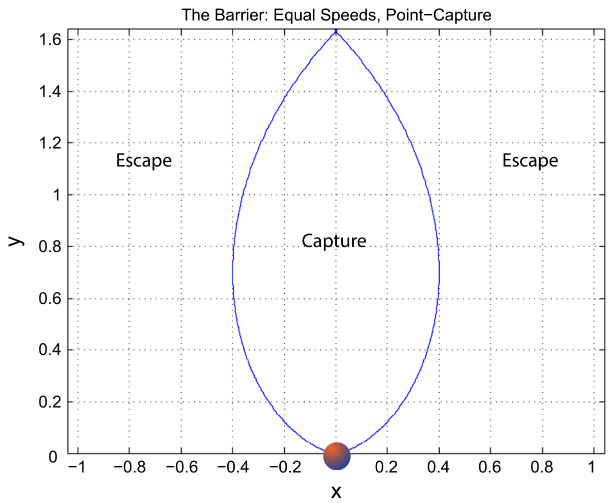

Fig. 6 The barrier, given by Eqs. (48) and (49), in the case of point-capture ($\ell = 0$), for $v_e = v_p = 1$ and $R = 0.7$

where $\bar{s}$ is given by (16) and $\tau_{\max}$ is the solution to the transcendental equation

$$v_p \tau_{\max} \sin(\bar{s} - c\tau_{\max}) = R - R\cos(c\tau_{\max}). \tag{50}$$

The barrier in this case is depicted in Fig. 6.

So far, we have solved a game of kind; specifically, we have characterized which states, under optimal play, lead to capture and which states lead to evasion. We now turn our attention to the time-optimal problem when the outcome is capture, that is, we shall consider initial states within the capture zone delineated by the barrier and examine the characteristics of the time-optimal capture trajectories. We will demonstrate that, for the special case of point-capture, the time optimal problem is equivalent to Zermelo's Navigation Problem in optimal control [34].

4 Point-capture: Time-Optimal Trajectories and Connection to Zermelo's Navigation Problem

Zermelo's Navigation Problem (ZNP) is a well-known result in optimal navigation, which has received a lot of attention in the literature (see for example [1,2,11]). Initially stated by the German mathematician Zermelo in 1931, the problem formally reads *In a given vector field of currents, which is a function of position (and possibly time), a vehicle moves with constant speed relative to the currents. How should the vehicle be navigated in order to reach a given destination in minimum time?* [5,34]. In ZNP, the equations of motion of the vehicle are given by

$$\dot{x} = v \cos\phi + U(x, y), \tag{51}$$
$$\dot{y} = v \sin\phi + Q(x, y), \tag{52}$$

where U, Q are known functions that correspond to the components of the vector field along the x and y directions, respectively, and ϕ is the heading angle with respect to the x-axis (the control input). The goal is to minimize time until the vehicle reaches a target location.

Returning to the original differential Eqs. (6)–(7), it is easy to observe that since E's optimal strategy is $u = -1$ (for initial conditions of the pursuer in the right-half plane), Eqs. (6) and (7) assume the form

$$\dot{x} = -v_p \sin\phi + \frac{v_e}{R} y, \tag{53}$$
$$\dot{y} = -v_p \cos\phi - \frac{v_e}{R} x - v_e, \qquad x \geq 0. \tag{54}$$

We may change the angle convention by introducing $\phi_z = 3\pi/2 - \phi$ to obtain

$$\dot{x} = v_p \cos\phi_z + \frac{v_e}{R} y, \tag{55}$$
$$\dot{y} = v_p \sin\phi_z - \frac{v_e}{R} x - v_e, \qquad x \geq 0, \tag{56}$$

and the target location which P intends to reach in minimum time is the origin (0, 0).

By comparing Eqs. (51)–(52) with (55)–(56), it is evident that E's optimal control results in an induced vector field akin to a current, which P needs to overcome in order to intercept E in minimum time. This vector field is shown in Fig. 7. This fact allows us to use the well-known *Zermelo's Navigation Formula* [5] which states that the optimal control ϕ^* obeys

$$\dot{\phi}^* = \sin^2\phi^* \frac{\partial Q(x, y)}{\partial x} + \sin\phi^* \cos\phi^* \left(\frac{\partial U(x, y)}{\partial x} - \frac{\partial Q(x, y)}{\partial y} \right) - \cos^2\phi^* \frac{\partial U(x, y)}{\partial y} \tag{57}$$

which, for $U(x, y) = v_e y/R$ and $Q(x, y) = -v_e x/R - v_e$, yields

$$\dot{\phi_z}^* = -\frac{v_e}{R}, \tag{58}$$

or, in terms of the initial angle ϕ of our problem,

$$\dot{\phi}^* = \frac{v_e}{R}. \tag{59}$$

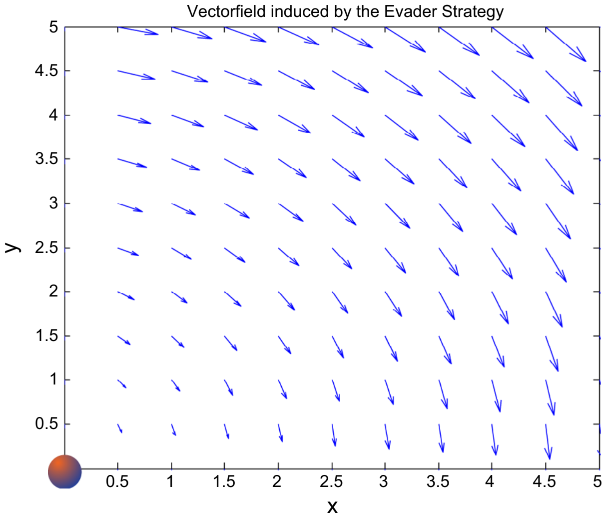

Fig. 7 Applying the evader's strategy induces a vector field that resembles a current, which P needs to overcome in order to intercept E in minimum time. *Plotted* for $v_p = v_e = 1$, $R = 0.7$

The problem therefore reduces to a two-point boundary value problem consisting of integrating equations (53), (54) and (59) subject to initial conditions (x, y) and $\phi^*(0)$ that will lead to a trajectory passing through the origin $(0, 0)$. Alternatively, one can consider integrating this system of ODEs backwards in time, i.e., by flipping the sign of the right-hand sides of (53), (54) and (59) and using the variable τ, subject to the retrograde boundary conditions $(x, y) = (0, 0)$ and a variable retrograde boundary condition $\phi_f^* \in [0,\ 2\pi]$ for (59). This will yield a parametric family of curves, and it remains to locate the one that passes through the original point (x, y) of interest. In fact, this integration can be performed analytically to obtain the following parametric family of curves:

$$x(\phi_f^*; \tau) = -R + R\cos(c\tau) + v_p\tau\sin(\phi_f^* - c\tau), \tag{60}$$

$$y(\phi_f^*; \tau) = R\sin(c\tau) + v_p\tau\cos(\phi_f^* - c\tau), \qquad \tau \in [0, \tau_{\max}], \tag{61}$$

where ϕ_f^* is the free parameter and $\tau_{\max}$ is the solution to the transcendental equation:

$$v_p\tau_{\max}\sin(\phi_f^* - c\tau_{\max}) = R - R\cos(c\tau_{\max}). \tag{62}$$

Figure 8 illustrates several time optimal trajectories, members of the parametric family of curves given by (60) and (61), corresponding to different values of ϕ_f^*. The barrier, i.e., the rightmost time optimal trajectory, is obtained for $\phi_f^* = \pi$ and is identical to the barrier of Sect. 3, shown in Fig. 6.

5 Optimal Trajectory in the Inertial Reference Frame

Although the pursuer control action leads to curved optimal paths in the reduced state space, as seen in Fig. 8, its trajectory in the inertial reference frame is a straight line. This can be easily seen from the fact that $\phi = \pi - \phi_p + \phi_e$, thus $\dot{\phi}_p = -\dot{\phi} + \dot{\phi}_e$ which, by virtue of the

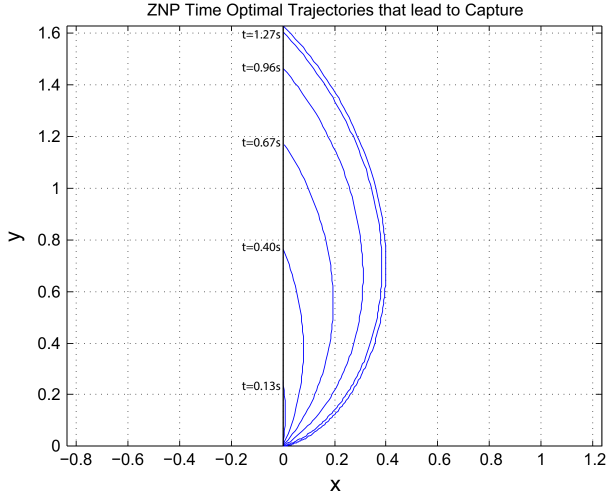

Fig. 8 Members of the parametric family of *curves* given by (60) and (61), corresponding to different values of ϕ_f^*, $v = 1$, $R = 0.7$. The time to capture is also shown for the case in which the game is initialized as a head-on engagement. For clarity, only the case $u^* = -1$ is shown. The *curves* for $u^* = 1$ are symmetric with respect to the y-axis

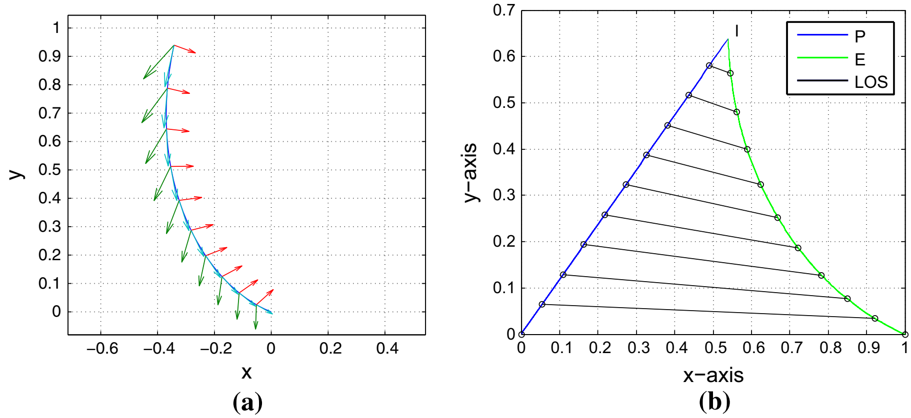

Fig. 9 **a** Optimal path in the reduced space of the evader fixed reference frame. *Arrows* indicate the players' controls (*green* for E and *red* for P) and the resulting motion direction (*blue*). **b** The resulting trajectory of motion depicted in (**a**), shown in the inertial reference frame. Optimal trajectories for P, E and evolution of the Line of Sight (LOS) (Color figure online)

ZNP solution of Eq. (59) and the evader dynamics given by Eq. (5) for $u = -1$, results in $\dot{\phi}_p^* = -v_e/R + v_e/R = 0$.

As a result, the intercept point I can be computed in closed form as shown in Figs. 9 and 10. Figure 9 shows an optimal path in the evader fixed reference frame and the resulting trajectories if the motion is translated into an inertial reference frame.

Figure 10 depicts the geometry of the problem in the inertial reference frame. For the sake of brevity, henceforth, we will continue the analysis for the case of equal speeds, although the same analysis can be performed for the more general case of unequal speeds. Given an initial distance L_0, for interception at point I, we have that $d_1 + d_2 = L_0$, where

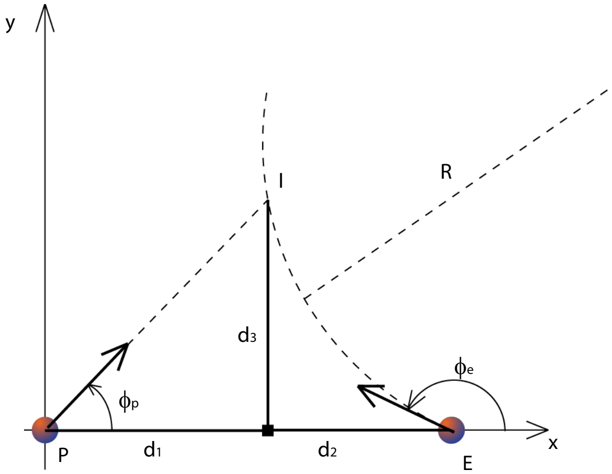

Fig. 10 Optimal Trajectories for P and E

$$d_1 = (v \cos \phi_p^*)\, t_f, \qquad d_2 = -\int_0^{t_f} -v \cos \phi_e(t)\, \mathrm{d}t,$$

and where $v = v_p = v_e$, which, combined with the following expression for d_3

$$d_3 = (v \sin \phi_p^*)\, t_f = \int_0^{t_f} v \sin \phi_e(t)\, \mathrm{d}t \tag{63}$$

yields

$$\begin{aligned} v t_f \cos \phi_p^* - \int_0^{t_f} v \cos(\phi_e(0) - v\, t/R)\, \mathrm{d}t &= L_0, \\ \int_0^{t_f} v \sin(\phi_e(0) - v\, t/R)\, \mathrm{d}t &= v\, t_f \sin \phi_p^*, \end{aligned}$$

or, alternatively,

$$v\, t_f \cos \phi_p^* = L_0 + R\big(\sin \phi_e(0) - \sin(\phi_e(0) - v t_f/R)\big), \tag{64}$$

$$v\, t_f \sin \phi_p^* = -R\big(\cos \phi_e(0) - \cos(\phi_e(0) - v t_f/R)\big). \tag{65}$$

Taking the squares of both sides of (64) and (65) and adding together yields

$$\begin{aligned} &v^2 t_f^2 + 2R^2 \cos(v t_f/R) + 2L_0 R \sin(\phi_e(0) - v t_f/R) \\ &-2L_0 R \sin \phi_e(0) - L_0^2 - 2R^2 = 0. \end{aligned} \tag{66}$$

This equation can be solved for t_f to find the optimal interception time. The optimal value ϕ_p^* is then given by (65) as follows:

$$\phi_p^* = \arcsin\left(\frac{R}{v t_f^*}\Big(-\cos \phi_e(0) + \cos(\phi_e(0) - \frac{v t_f^*}{R})\Big)\right), \qquad \phi_p^* \in [0, \frac{\pi}{2}], \tag{67}$$

where t_f^* denotes the optimal interception time. It is important to note that the above equations are only valid if the initial state of the game lies within the capture region of Fig. 6.

6 Domain Decomposition in the Case of a Faster Pursuer

For the sake of completeness, in this section we investigate the case when the pursuer is not only completely agile, but is also faster than the evader (that is, the speed ratio $\alpha = v_p/v_e > 1$). As already stated, this case leads to global capturability, namely, the evader is captured regardless of the initial conditions of the pursuer and the evader [6]. Although capture is guaranteed on the entire Euclidean plane, it is shown below that the Euclidean plane can be partitioned by a boundary $\mathcal{B}$ separating two different types of solutions exhibited in the game: one in which the evader is captured while performing a hard turn, and another one in which the evader, having completed the turn, is captured during a straight-line dash while trying to avoid the pursuer (also referred to as the *end game*). The region inside the boundary $\mathcal{B}$ encloses the circular target set and corresponds to initial conditions that lead to the first type of solution. For initial conditions of the game outside of the boundary, the second type of solution manifests itself. The shape of the boundary $\mathcal{B}$ resembles in appearance the one of the barrier for the case $\alpha \leq 1$. A geometric procedure to obtain the boundary $\mathcal{B}$ in the *realistic plane* is presented next.

6.1 Geometric Construction of the Boundary in the Inertial Reference Frame

Recall that the optimal trajectory of the pursuer is a straight line in the inertial reference frame. Points on the boundary correspond to initial conditions of the pursuer so that capture occurs at the end of the evader's turning maneuver. To this end, let the inertial reference frame whose origin coincides with the *initial* position of the evader and the y-axis coincides with the evader's initial velocity vector orientation (see Fig. 11). From the point centered at $O = (-R, 0)$, draw a circle of radius R. For each $\theta \in [0, \theta_{\max}]$, draw the tangent to the circle of radius R centered at O of length $\alpha R\theta + \ell$, from the point $E'(\theta)$ on the circle, as shown in Fig. 11. The endpoint B of the tangent line lies on $\mathcal{B}$, and as θ ranges from $\theta = 0$ to $\theta = \theta_{\max}$ the point B traces the boundary $\mathcal{B}$.

Note that $\theta_{\max}$ is given by the solution to the transcendental equation:

$$\tan\frac{\theta_{\max}}{2} = \alpha\theta_{\max} + \frac{\ell}{R}, \tag{68}$$

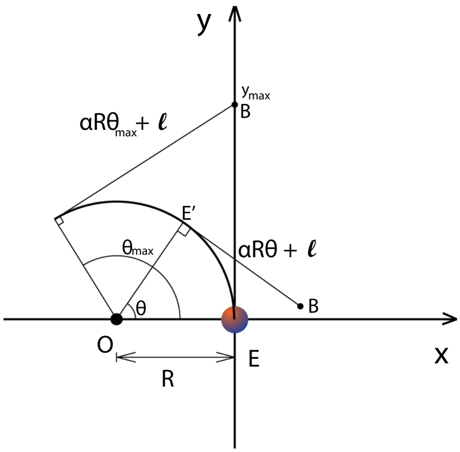

Fig. 11 The construction of the boundary $\mathcal{B}$

and when $\theta = 0$, then $B = (0, -\ell)$ and the boundary $\mathcal{B}$ meets the y-axis at $y_{\max} = \alpha R\theta_{\max} + \ell$.

In the case of point-capture ($\ell = 0$), Eq. (68) reduces to

$$\tan \frac{\theta_{\max}}{2} = \alpha\theta_{\max}, \tag{69}$$

where $\theta_{\max} > \pi/2$. The boundary $\mathcal{B}$ then meets the y-axis at $y_{\max} = \alpha R\theta_{\max}$. When point-capture is considered, the boundary $\mathcal{B}$ is the *involute* of the circle of radius R centered at O, that is, it is the curve obtained by attaching a taut string of length $R\theta_{\max}$ to the point $E'(\theta_{\max})$ on the circumference of the circle of radius R centered at O, and tracing its free end as it unwinds.

In Cartesian coordinates, the involute is obtained geometrically from Fig. 12 as follows:

$$x(\theta)/R = \cos\theta + \alpha\theta \sin\theta - 1, \tag{70}$$

$$y(\theta)/R = \sin\theta - \alpha\theta \cos\theta. \tag{71}$$

The boundary in this case is depicted in Fig. 13.

Fig. 12 The construction of the boundary $\mathcal{B}$ for point-capture

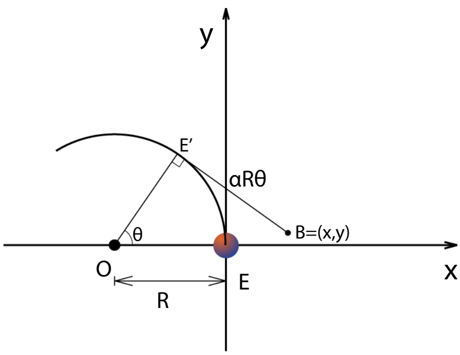

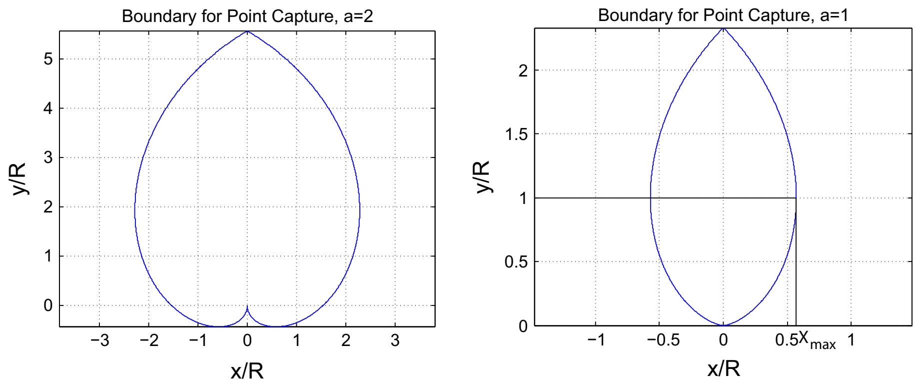

(a) **(b)**

Fig. 13 The boundary $\mathcal{B}$ in the case of point capture, for **a** $\alpha = 2$, and **b** $\alpha = 1$. Notice that in (**b**), $x_{\max}/R$ corresponds to $y/R = 1$ and is equal to $\pi/2 - 1$. For $\alpha > 1$ the area enclosed by these *curves* corresponds to initial conditions that lead to capture while the evader is turning, whereas initial conditions outside the area enclosed by the *curve* lead to capture after the evader has completed her turn and while she performs a *straight-line dash* away from the evader (end game). For $\alpha = 1$, this *curve* separates the regions of capture (*inside*) and escape (*outside*), and it thus coincides with the barrier shown in Fig. 6

6.2 The End Game Solution in an Inertial Reference Frame

The case of capture by a faster pursuer when the game exhibits a tail chase admits a geometric solution similar to the one presented in Sect. 5. Assume that the pursuer is positioned at an initial distance d from the evader, as shown in Fig. 14. In the resulting trajectory, the evader completes a hard turn and is captured after a tail chase at point I. According to Fig. 14, which depicts the case when the evader initial position is in the lower right quadrant (that is, when $\beta \geq \pi/2$), and recognizing that $d = \sqrt{x^2 + y^2}$, $\sin\beta = x/d$ and $\cos\beta = y/d$, one directly obtains

$$OP = \sqrt{d^2 + R^2 + 2Rd\sin\beta}, \tag{72}$$

$$E'P = \sqrt{d^2 + 2Rd\sin\beta}, \tag{73}$$

$$\cos(\delta + \theta) = \frac{R}{OP}, \tag{74}$$

$$\sin(\delta + \theta) = \frac{E'P}{OP}, \tag{75}$$

$$\sin\delta = -\frac{d\cos\beta}{OP}, \tag{76}$$

$$\cos\delta = \frac{R + d\sin\beta}{OP}. \tag{77}$$

Applying well-known trigonometric formulas, Eqs. (72)–(77) result in the following expression for θ:

$$\sin\theta = \frac{(R + d\sin\beta)\sqrt{d^2 + 2Rd\sin\beta} + Rd\cos\beta}{d^2 + R^2 + 2Rd\sin\beta}, \tag{78}$$

$$\cos\theta = \frac{-d\cos\beta\sqrt{d^2 + 2Rd\sin\beta} + R(R + d\sin\beta)}{d^2 + R^2 + 2Rd\sin\beta}. \tag{79}$$

A similar analysis can be performed if the pursuer's initial position is in the upper right quadrant, that is, when $\beta < \pi/2$. In this case, one simply has to replace the angle $\theta + \delta$ with the angle $\theta - \delta$ in Eqs. (74)–(75), and change Eq. (76) to $\sin\delta = d\cos\beta/OP$. Solving the resulting systems yields the same expressions for $\sin\theta$ and $\cos\theta$, namely Eqs. (78)–(79).

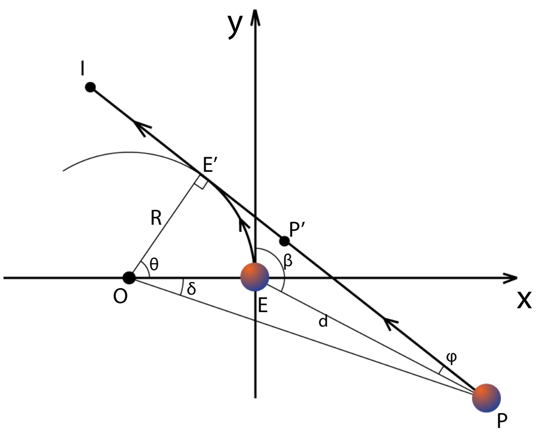

Fig. 14 The end game solution in the inertial reference frame centered at the evader's initial position, aligned with the evader's initial velocity vector. The point P' denotes the location of the pursuer at the end of the evader's turning maneuver (that is, when the evader is at point E')

The optimal control of the pursuer expressed in relative bearing with respect to the line of sight, as shown in Fig. 14, is readily obtained as $\varphi^* = \pi - \beta - \theta$. The time to capture can be computed to be

$$t_f = \frac{E'P' - \ell}{v_p - v_e} + \frac{R\theta}{v_e}, \tag{80}$$

where P' is the location of the pursuer when the evader is at location E'. Noticing that $E'P' = E'P - \alpha R\theta$, the above expression finally yields

$$t_f = \frac{\sqrt{d^2 + 2Rd\sin\beta} - \alpha R\theta - \ell}{v_p - v_e} + \frac{R\theta}{v_e}. \tag{81}$$

7 Conclusions

In this paper, we have investigated the pursuit and evasion differential game between an agile pursuer and an evader having maneuverability restrictions, that is, a "pedestrian" and a "car" á la Isaacs, respectively. The agents are assumed to have constant speeds. There are two problem parameters, namely the speed ratio $\alpha = v_p/v_e$ and the turn and capture radius ratio ℓ/R. Using the framework of differential game theory, it was proven that the evader's optimal strategy is to always initially make a hard turn away from the pursuer irrespective of the problem parameters, while the pursuer's optimal strategy is to hold a fixed course; if $\alpha > 1$ and initially P is far from E the endgame will entail a pure pursuit.

The solution of the game entails a characterization of the barrier that separates states that lead to capture under optimal play, and states that lead to evasion regardless of the pursuer's actions. For a speed ratio $\alpha = v_p/v_e \leq 1$, the capture region is bounded. The speed ratio $\alpha > 1$ leads to global capture but, unlike in the Homicidal Chauffeur differential game, there is no open barrier and the evader does not perform a swerve maneuver. Time-optimal trajectories were obtained by recognizing the equivalence of this problem, when point-capture is investigated, to the classical Zermelo navigation problem in optimal control. The equivalent analysis of the problem in the inertial frame allows the explicit calculation of the time of capture and the corresponding optimal pursuer (constant) inertial heading. Apart from their own intrinsic differential game theoretic merit, the results of this paper have immediate application to collision avoidance problems. Specifically, the barrier delineates a safe region in which a collision is not possible even in the worst case of a malicious—and more agile—pursuer. The application of the results of this paper in two-agent and multi-agent collision avoidance problems, such as Air Traffic Control and maritime collision avoidance, are currently under investigation and will be reported in the near future.

Acknowledgments This work was supported in part by the AFOSR Award No. FA9550-13-0029 and NSF Award No. CMMI-1160780. The first author also gratefully acknowledges support from the A. S. Onassis Public Benefit Foundation.

References

1. Bakolas E, Tsiotras P (2010) Time-optimal synthesis for the Zermelo–Markov–Dubins problem: the constant wind case. In Poceedings of the American control conference, Baltimore, MD, pp 6163–6168
2. Bakolas E, Tsiotras P (2012) Feedback navigation in an uncertain flowfield and connections with pursuit strategies. J Guid Control Dyn 35(4):1268–1279
3. Basar T, Olsder GJ (1995) Dynamic noncooperative game theory. Academic Press, Waltham

4. Bopardikar S, Bullo F, Hespanha J (2007) A cooperative homicidal chauffeur game. In Proceedings of the 46th IEEE conference on decision and control pp 4857–4862
5. Bryson A, Ho Y (1975) Applied optimal control: optimization, estimation and control. Taylor and Francis, New York
6. Cockayne E (1967) Plane pursuit with curvature constrains. SIAM J Appl Math 15:1511–1516
7. Exarchos I, Tsiotras P (2014) An asymmetric version of the two car pursuit-evasion game. In Proceedings of the 53rd IEEE conference on decision and control, Los Angeles, CA
8. Ho Y, Bryson A, Baron S (1965) Differential games and optimal pursuit-evasion strategies. IEEE Trans Autom Control 10:385–389
9. Isaacs R (1965) Differential games. Willey, New York
10. Lewin J (1994) Differential games—theory and methods for solving game problems with singular surfaces. Springer, London
11. Li B, Xu C, Kok LT, Chu J (2013) Time optimal Zermelo's navigation problem with moving and fixed obstacles. J Appl Math Comput 224:866–875
12. Meier LI (1969) A new technique for solving pursuit-evasion differential games. IEEE Trans Autom Control 14(4):352–359
13. Merz A (1971) Homicidal chauffeur-a differential game. Ph.D. Thesis, Stanford University
14. Merz A (1972) The game of two identical cars. J Opt Theory Appl 9:324–343
15. Merz A (1973) Optimal evasive maneuvers in maritime collision avoidance. J Inst Navig 20(2):144–152
16. Miloh T, Sharma SD (1975) Bericht nr. 319: determination of critical maneuvers for collision avoidance. Tech Rep, Institut fur Schiffbau, Technische Universitat Hamburg
17. Miloh T, Sharma SD (1976) Bericht nr. 329: maritime collision avoidance as a differential game. Tech Rep, Institut fur Schiffbau, Technische Universitat Hamburg
18. Mitchell I (2001) Games of two identical vehicles. Technical Report, Department of Aeronautics and Astronautics (SUDAAR), Stanford University, Stanford, CA
19. Mitchell I, Bayen A, Tomlin C (2005) A time-dependent Hamilton–Jacobi formulation of reachable sets for continuous dynamic games. IEEE Trans Autom Control 50:947–957
20. Nahin PJ (2007) Chases and escapes: the mathematics of pursuit and evasion. Princeton University Press, Princeton
21. Olsder GJ, Walter JL (1977) Collision avoidance of ships. Tech Rep, Dept of Applied Mathematics, Twente University of Technology
22. Olsder GJ, Walter JL (1977) A differential game approach to collision avoidance of ships. Optimization techniques. Lecture notes in control and information sciences, vol 6. Springer, Berlin pp 264–271
23. Pachter M (2002) Simple-motion pursuit-evasion differential games. In Proceedings of the 10th Mediterranean conference on control and automation
24. Pachter M, Miloh T (1987) The geometric approach to the construction of the barrier surface in differential games. Comput Math Appl 13(1–3):47–67
25. Pachter M, Yavin Y (1981) A stochastic homicidal chauffeur pursuit-evasion differential game. J Opt Theory Appl 34(3):405–424
26. Patsko V, Turova V (2001) Level sets of the value function in differential games with the homicidal chauffeur dynamics. Int Game Theory Rev 3(1):67–112
27. Pshenichnyi B (1976) Simple pursuit by several objects. Kibernetika 3:145–146
28. Rublein G (1972) On pursuit with curvature constrains. SIAM J Control 10:37–39
29. Salmon D (1969) Policies and controller design for a pursuing vehicle. IEEE Trans Autom Control 14(5):482–488
30. Sgall J (2001) Solution of David Gale's lion and man problem. Theoret Comput Sci 259(1–2):663–670
31. Vincent TL, Peng WY (1973) Ship collision avoidance. In Proceedings of the workshop on differential games, Naval Academy, Annapolis
32. Yavin Y (1986) Stochastic pursuit-evasion differential games in the plane. J Opt Theory Appl 50:495–523
33. Yavin Y, Villiers RD (1989) Proportional navigation and the game of two cars. J Opt Theory Appl 62:351–369
34. Zermelo E (1931) Uber das Navigationsproblem bei ruhender oder veranderlicher Windverteilung. Zeitschrift fuer Angewandte Mathematik und Mechanik 11:114–124